Development and Validation of an Improved Neurological Hemifield Test to Identify Chiasmal and Postchiasmal Lesions by Automated Perimetry

Allison N. McCoy,[1] Harry A. Quigley,[1,2] Jiangxia Wang,[3] Neil R. Miller,[4] Prem S. Subramanian,[4] Pradeep Y. Ramulu,[1,2] and Michael V. Boland[1,5]

[1]Glaucoma Center of Excellence, Wilmer Eye Institute, Johns Hopkins University, Baltimore, Maryland
[2]Dana Center for Preventive Ophthalmology, Wilmer Eye Institute, Johns Hopkins University, Baltimore, Maryland
[3]Department of Biostatistics, Johns Hopkins School of Public Health, Baltimore, Maryland
[4]Neuro-Ophthalmology Service, Wilmer Eye Institute, Johns Hopkins University, Baltimore, Maryland
[5]Division of Health Sciences Informatics, Johns Hopkins University, Baltimore, Maryland

Correspondence: Michael V. Boland, 600 N Wolfe Street, Wilmer 131 Baltimore, MD 21287; boland@jhu.edu.

Submitted: December 2, 2013
Accepted: January 6, 2014

Citation: McCoy AN, Quigley HA, Wang J, et al. Development and validation of an improved neurological hemifield test to identify chiasmal and postchiasmal lesions by automated perimetry. *Invest Ophthalmol Vis Sci*. 2014;55:1017–1023. DOI:10.1167/iovs.13-13702

Purpose. To improve the neurological hemifield test (NHT) using visual field data from both eyes to detect and classify visual field loss caused by chiasmal or postchiasmal lesions.

Methods. Visual field and clinical data for 633 patients were divided into a training set (474 cases) and a validation set (159 cases). Each set had equal numbers of neurological, glaucoma, or glaucoma suspect cases, matched for age and for mean deviation between neurological and glaucoma cases. NHT scores as previously described and a new NHT laterality score were calculated. The ability of these scores to distinguish neurological from other fields was assessed with receiver operating characteristic (ROC) analysis. Three machine classifier algorithms were also evaluated: decision tree, random forest, and least absolute shrinkage and selection operator (LASSO). We also evaluated the ability of NHT to identify the type of neurological field defect (homonymous or bitemporal).

Results. The area under the ROC curve (AUC) for the maximum NHT score was 0.92 (confidence interval [CI]: 0.87, 0.97). Using NHT laterality scores from each eye combined with the sum of NHT scores, the AUC improved to 0.93 (CI: 0.88, 0.98). The largest AUC for machine learning algorithms was for the LASSO method (0.96, CI: 0.92, 0.99). The NHT scores identified the type of neurological defect in 96% (158/164) of patients.

Conclusions. The new NHT distinguished neurological field defects from those of glaucoma and glaucoma suspects, providing accurate categorization of defect type. Its implementation may identify unsuspected neurological disease in clinical visual field testing.

Keywords: glaucoma, visual field, neurological disease, neuro-ophthalmology, chiasm, homonymous, bitemporal, algorithm

Automated visual field testing is important in the diagnosis and management of diseases affecting the optic nerve and visual pathway. A number of algorithms are now present in commercial products to assist clinicians in the interpretation of perimetry results, such as those implemented on the Humphrey Field Analyzer (HFA; Carl Zeiss Meditec, Dublin, CA), including the mean deviation (MD), pattern standard deviation (PSD), visual field index (VFI), and glaucoma hemifield test (GHT).[1,2] Additional investigational approaches to the analysis of field data and field progressive worsening have been reported using artificial neural networks analysis[3–8] and predictive models.[9,10]

We previously described an algorithm called the neurological hemifield test (NHT) to improve the detection of chiasmal and postchiasmal visual field loss.[11] The NHT is based on the tendency for neurological disease at or posterior to the chiasm to produce visual field defects that affect one side of the vertical midline more than the other. This results from the typical segregation at the chiasm of retinal ganglion cell (RGC) axons arising nasal and temporal to a vertical line through the fovea, with minor exceptions.[12] These chiasmal and postchiasmal neurological visual field defects can be classified as right or left homonymous when the same side is affected in each eye, or as bitemporal or binasal. While binasal defects occur rarely in neurological disease, defects of both nasal field areas are more characteristic of glaucomatous neuropathy, though these do not typically respect the vertical midline.

The NHT uses pointwise data from the pattern deviation analysis of the HFA instrument, much as the GHT compares pointwise pattern deviation data from mirror image clusters across the horizontal field meridian.[13,14] The power of GHT analysis to identify glaucoma injury derives from the tendency of glaucoma damage to affect the upper field differently from the lower field due to segregation of upper and lower RGC axons at the optic disc. In developing the initial NHT, we found a high sensitivity and specificity when comparing one group of 16 points in the left hemifield to the mirror image 16 points in the right hemifield, separated by the vertical midline. Thus, while the GHT compares any one or more of five clusters of

Table 1. Patient Demographics by Diagnosis

	Neurological, $n = 211$	Glaucoma, $n = 211$	Suspects, $n = 211$	*P* Value: Glaucoma vs. Neurological	*P* Value: Suspects vs. Neurological	Neurological Diagnoses
Age	54.3 ± 16.2	56.9 ± 14.7	53.8 ± 16.1	0.09	0.75	
MD maximum	−7.3 ± 6.4	−7.0 ± 6.2	−1.0 ± 2.5	0.49	<0.0001	
MD minimum	−10.6 ± 7.7	−10.4 ± 8.1	−2.6 ± 3.9	0.82	<0.0001	
MD mean	−9.0 ± 6.9	−8.7 ± 7.0	−1.8 ± 3.1	0.66	<0.0001	
Stroke						72
Chiasmal syndrome/tumor						55
Tumor						44
Vascular malformation						13
Trauma						6
Alzheimer disease						4
Demyelinative disease						4
Unknown cause						4
Optic tract lesion						3
Infection						2
Aneurysm						2
Hydrocephalus						1
Neurosurgical procedure						1

three to six points to each other, the NHT uses only a single, larger cluster for comparison.

Our initial assessment of the NHT utilized the maximum NHT score from the two eyes of a given subject to identify defects that differed between the right and left hemifield. Even this essentially monocular NHT rivaled the performance of glaucoma and neuro-ophthalmology subspecialists who graded the right and left eye data of the same patients to categorize fields as either neurological or glaucomatous. To improve the NHT further, we developed methods to analyze the visual field data from both eyes of each patient with two goals: first, to determine whether the inclusion of these data is helpful in identifying a neurological pattern of damage; and second, to categorize the pattern as either right/left homonymous or bitemporal. We also assessed the performance of three machine learning classifiers using NHT values as inputs.

Methods

Patient Selection

This research was reviewed and approved by the Institutional Review Board of the Johns Hopkins University School of Medicine and abided by the tenets of the Declaration of Helsinki. Visual field test results were identified from existing records of patients at the Wilmer Ophthalmological Institute, Johns Hopkins School of Medicine. Among 633 pairs of bilateral field tests, one-third were from patients with a chiasmal or postchiasmal lesion causing a bitemporal or a homonymous field defect seen by Wilmer neuro-ophthalmologists from 1999 to 2012 (Tables 1, 2). Visual fields were selected for inclusion based upon their reliability indices, with the most reliable set of fields chosen for each subject. Any studies in which only one eye was tested were excluded. When multiple pairs of reliable fields were available for a given patient, we chose the pair of fields with the subtlest defect as determined by the lowest PSD value. The fields were not filtered based upon the specific pattern of field loss, whether complete or incomplete, congruous or incongruous. Junctional scotomas were included. The clinical diagnosis and field type were confirmed by a neuro-ophthalmologist (NRM or PSS) from the history, examination, and neuroimaging studies.

Glaucoma and glaucoma suspect fields were selected from a database of visual fields from Wilmer Glaucoma Center of Excellence patients seen from 1999 to 2007. We have previously validated the diagnosis of glaucoma by chart review of clinical data.[15] The fields of glaucoma suspects were used for comparison with glaucoma and neurological patients because the testing of such suspects is a frequent reason for performing perimetry. Therefore, they represent a realistic control group for field tests occurring in the clinical setting among whom unsuspected neurological disease might be useful to identify.

For each neurological patient, we matched one glaucoma and one glaucoma suspect case by age. In addition, we required both the right and left visual fields from the glaucoma subject to have an MD within 30% of the same eye in the neurological field pair. Differences between neurological and glaucoma/glaucoma suspect patients by age were not significantly different, by design (Table 1). Likewise, the MD values of neurological and glaucoma patients were also insignificantly different by design. The pointwise pattern deviation values from each visual field were then used to calculate the NHT score as described below.

The overall group of patients was expanded from the 276 patients in our initial report[11] to a total of 633 patients. In order to divide the patients into a training set and a validation set for use with the machine learning classifiers, we placed three patients in the training set for each patient in the validation set, as suggested in prior publications.[16]

Table 2. Patient Distribution by Diagnosis in Training and Validation Sets

	Training Set, *n* (%)	Validation Set, *n* (%)
All	474	159
Glaucoma or glaucoma suspects	316 (67)	106 (67)
Neurological patients	158 (33)	53 (23)
Neurological diagnoses		
Bitemporal	43 (27)	12 (23)
Homonymous	115 (73)	41 (77)

The neurological patient fields were classified by type (bitemporal, right or left homonymous) by one of two neuro-ophthalmologists and were each consistent with the clinical findings of the patient as to location of their central nervous system disease.

Calculation of the NHT score

The NHT score was calculated as previously described from scores assigned to the pattern deviation values of individual field test points, grouped into two clusters on either side of the vertical midline (Fig. 1). The NHT patterns do not include points near the blind spot nor points in the nasal field that are typically affected in glaucoma. In brief, the NHT score assigned to each eye is calculated as the absolute value of the difference between the sum of pointwise scores between these two regions. Hence, if the pattern deviation values were normal on both sides or equally abnormal on both sides, the score would be low, while the greater the numerical value of the NHT, the higher the likelihood of chiasmal or postchiasmal disease.

To improve on our prior algorithm, we now define the NHT laterality score as the difference between the scores of the right and left NHT regions in the visual field of a given eye, retaining the positive or negative sign of the value (Fig. 1). Since this value retains its sign, it is intended to distinguish bitemporal from homonymous neurological damage. A person with homonymous defects, for instance, will have NHT laterality scores that have the same sign in both eyes, with recognition of right or left homonymous by whether the sides that are positive or negative are in the right or left halves of the fields. Bitemporal defects would have NHT laterality scores of opposite signs in the two eyes.

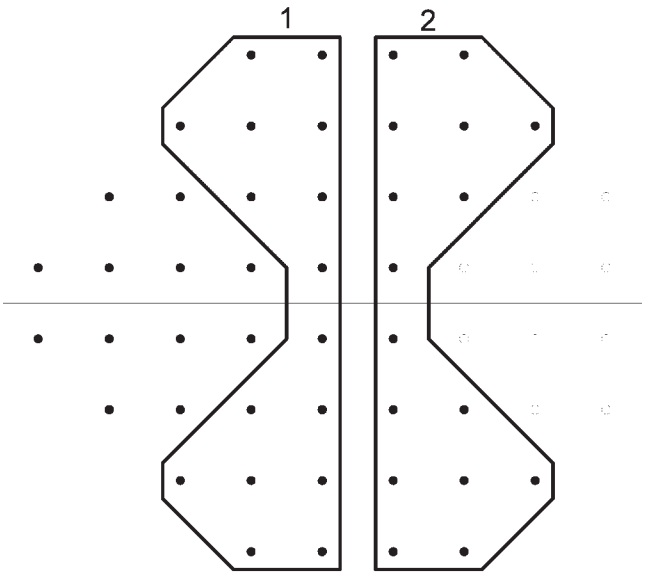

FIGURE 1. Clusters of visual field points compared by the NHT, on either side of vertical midline, shown here outlined as dumbbell-shaped regions in a right eye, 24-2 pattern. Scores proportional to the depth of the defect are calculated for each point and then summed for each region. Overall scores are then calculated as the difference between nasal and temporal hemifields, either maintaining the sign (NHT laterality score) or calculating the absolute value (NHT score). *Open circles* indicate the points that fall in or near the blind spot, and which are not included.

Construction of Models to Evaluate the New NHT

ANOVA was used to compare age, MD, PSD, and NHT scores between diagnosis groups. ANOVA was also used to evaluate differences between the three types of neurological disease: bitemporal, left homonymous, and right homonymous. The GHT asymmetry was also compared among the neurological patients using Fisher's exact test.

Receiver operating characteristic analysis was used to evaluate the performance of each model with regard to distinguishing subjects with neurological visual field defects from those either diagnosed as glaucoma or as a glaucoma suspect. The first classifier tested was logistic regression using combinations of the single eye NHT scores as inputs (maximum value between the two eyes, minimum value, mean value, and sum of two absolute values). In addition, we compared neurological with glaucoma/glaucoma suspect groups in logistic models using the two NHT laterality scores from a given subject combined with the previously defined NHT score (absolute value). Models were created using the training set of 474 patients, and then tested using the validation set of 159 patients.

We additionally evaluated three machine learning algorithms as methods to distinguish neurological visual field defects from those of glaucoma/glaucoma suspects. In this analysis, we included not only the NHT scores from the point cluster comparison groups in Figure 1, but also scores calculated from six additional mirror image clusters that included either fewer or more points than the standard cluster. An NHT score was calculated for each of the six additional patterns for each eye using the pattern deviation values for the standard pattern, as well as only the superior or inferior points for each of these clusters. The absolute cross-vertical difference in the sum of these values was the NHT score. In addition to the NHT score and NHT laterality scores, other candidate variables were provided to the algorithms, including the individual pattern deviation values, the probability of pattern deviation values, total deviation values, and the between eye difference of the deviation values at each point using the symmetric coordinates. These candidate-independent variables were assessed in the following three models, developing their algorithm in the training data set of 474 patients, and then testing it in the validation set of 159 patients.

Model one was a decision tree model,[17] which follows a recursive algorithm that identifies a variable that best splits the data into two groups. This process is then applied separately to each subgroup recursively until the subgroups either reach a minimum size or until no further improvement can be made. The resulting model is represented as binary trees. Model two was a random forest model[18] created by the generation of multiple decision trees, each giving a classification. The model chooses the decision tree, or classification, that shows up most frequently. Model three was the least absolute shrinkage and selection operator (LASSO),[19] a logistic regression model. Here, the variables related to total deviation and pattern deviation were not included because they are highly correlated with variables generated from the probability of pattern deviation. LASSO is a regression method that involves penalizing the absolute size of the regression coefficients. As a result, some of the parameter estimates may be exactly zero. The larger the penalty applied, the further the estimates are shrunk toward zero. The areas under ROC curves from different models were compared using the method of DeLong et al.[20]

The analyses were performed with statistical software (Stata version 12.1; StataCorp, College Station, TX; and R version 2.15.3; R Development Core Team, University of Auckland, Auckland, New Zealand), with the rpart, randomForest, and glmnet packages. P values ≤ 0.05 were considered statistically significant.

Results

Our previous analysis found an AUC for the maximum NHT score of 0.90 (confidence interval [CI]: 0.86, 0.94). A maximum NHT score of 30 or more had a sensitivity of 87% (CI: 78%, 93%) and specificity of 73% (CI, 66%–79%). Examples of visual field test results and their maximum NHT scores for the current data set are shown in Figure 2.

To allow evaluation of the machine learning classifiers, we mixed two sets of matched neurological—glaucoma—glaucoma suspect triplets into two: a training set and a validation set. The AUCs for the maximum NHT score and the sum of NHT scores were similar to those previously determined with the smaller published dataset (Table 3). The highest AUC was for a model in which both the sum of NHT scores and the NHT laterality score for right and left eyes were included (significantly better than the sum of NHT scores alone for training set, $P < 0.001$, χ^2 test).

The machine learning algorithms also had high AUC values for separating neurological visual fields from glaucoma and glaucoma suspect visual fields (Table 4). However, the AUC of the decision tree, random forest, and LASSO algorithms did not differ significantly from that of the logistic model of NHT sum and laterality values ($P = 0.055$, χ^2 test), though their values were generally somewhat higher.

The range of sensitivity versus specificity values for particular values of the maximum NHT score showed 89% sensitivity and 72% specificity for a score of 30, 83%/91% at a score of 50, and 75%/98% for a value of 70 (Table 5). The positive predictive value (PPV) ranged from 62% using a maximum NHT score of 30 to 95% for a maximum NHT score of 70. The negative predictive value (NPV) ranged from 93% to 89% at these cutoffs, respectively.

We also sought to determine the ability of the NHT laterality score to identify the specific type of neurological defect. The first step in this process was to use a cutoff for the maximum NHT score that would be a reasonable mix of sensitivity and specificity. Using the score of 50 among all cases in both datasets, 44/53 (83%) were correctly classified as neurological patients (Table 6). Among the nine neurological patients that were not captured by the cutoff, three (33%) were bitemporal, four (45%) were left homonymous, and two (22%) were right homonymous. With a maximum NHT score of 70 as the dividing line, the correct differentiation of neurological cases from glaucoma and glaucoma suspect cases was not substantially different from that of a score of 50 (Table 6).

One of the primary goals of this work was to enhance our prior algorithm by classifying the pattern of neurological field loss as bitemporal, right homonymous, left homonymous, or binasal. These classifications were then compared with the true clinical diagnosis. Among the training and validation datasets combined, there were only six misclassifications for the 164 neurological patients with the maximum NHT score $\geq$ 50 (Table 7). There was near-perfect identification of the homonymous hemianopic types, while five bitemporal cases were classified as right homonymous and one left homonymous was classified as binasal. Among the 51 glaucoma and glaucoma suspect patients with a maximum NHT score $\geq$ 50, seven were diagnosed as bitemporal, nine as left homonymous, and six as right homonymous; 29 were binasal.

Discussion

We developed the NHT to aid clinicians in the recognition of neurological patterns in visual fields for patients in whom such defects might not otherwise have been noticed. In the original report, in which we used the maximum NHT value between the two eyes of a subject, the metric performed similarly to experienced clinicians in the separation of neurological from glaucoma or glaucoma suspect fields. The present report extends that evaluation of the NHT by generating a method in which data from both eyes are included in the analysis in order to identify the type of neurological field defect pattern (homonymous, bitemporal). We also improved on our prior analysis by including new cases and by evaluating the performance of machine learning classifiers. The higher the NHT score for a given pair of visual fields, the more likely that neurological disease is to be the cause of the field findings.

In practical usage, the "ideal" ROC value may not be that which most serves the pragmatic purpose of the NHT score. We envision the NHT approach to be one in which clinicians who are performing visual field testing for the most common reason—identification of glaucomatous visual field loss—will be alerted to an unexpected neurological defect in the field test. If this is to be the purpose, then one would not choose a criterion that is the most sensitive to neurological defects, nor the point on the ROC curve closest to the (0,1) point on the plot, but rather a criterion that is reasonably sensitive to neurological findings, but highly specific. One should not be unduly alarmed about the possibility that there is a neurological defect when the chance is very low. Thus, a maximum NHT score in the range of 70 would seem appropriate to keep the chance of false-positive alerting to central nervous system disease below 2% to be the most useful. This threshold also provides a reasonable positive predictive value of 95%. However, there may be a role for providing the NHT score in more subtle cases as a borderline finding meriting further history or examination.

It was gratifying that the specific categorization of the type of neurological defect was highly accurate (e.g., bitemporal, homonymous right/left). While not perfect, this method would point the clinician to some degree toward the proper location for topographical diagnostic testing and etiology. While some glaucoma eyes were above the NHT score criterion as neurological, it is reassuring that more than 60% of these were binasal defects. There are occasional neurological diseases, such as dolichoectatic carotid arteries that give binasal defects, but glaucoma is the overwhelmingly dominant reason for such defects. Thus, the specificity of the topographical characterization of our binocular NHT algorithm not only helps to identify such defects, but also gives their type.

We also evaluated three machine classifier algorithms as methods to identify neurological field pattern as distinct from glaucoma/glaucoma suspect. The LASSO method had the highest AUC of all methods studied. While there were slightly higher values of the AUC in ROC analysis for these methods, there was no statistically significant increase in their predictive value over the simpler NHT parameter. It might be considered that these methods are more complicated to implement, since they have multiple inputs from the field data. However, once the coding to generate this large number of inputs is written, the methods are rapidly implementable. As in other such algorithms, however, the specific values that lead to segregation of neurological from non-neurological field findings are not easily extracted.

While the NHT is promising for clinical use in detecting chiasmal and postchiasmal field defects, the test was not designed to replace clinician judgment. Additional clinical data, including visual acuity, color vision, ophthalmoscopic appearance, and historical information, must be used to assist in this differentiation. The NHT will also identify as abnormal visual field defects produced by patients who intentionally simulate quadrantanopia, hemianopia, and bitemporal defects.[21] Due to the protocol for threshold testing with the HFA instrument, a subject who fails to respond to stimuli at the cardinal point in

Investigative Ophthalmology & Visual Science

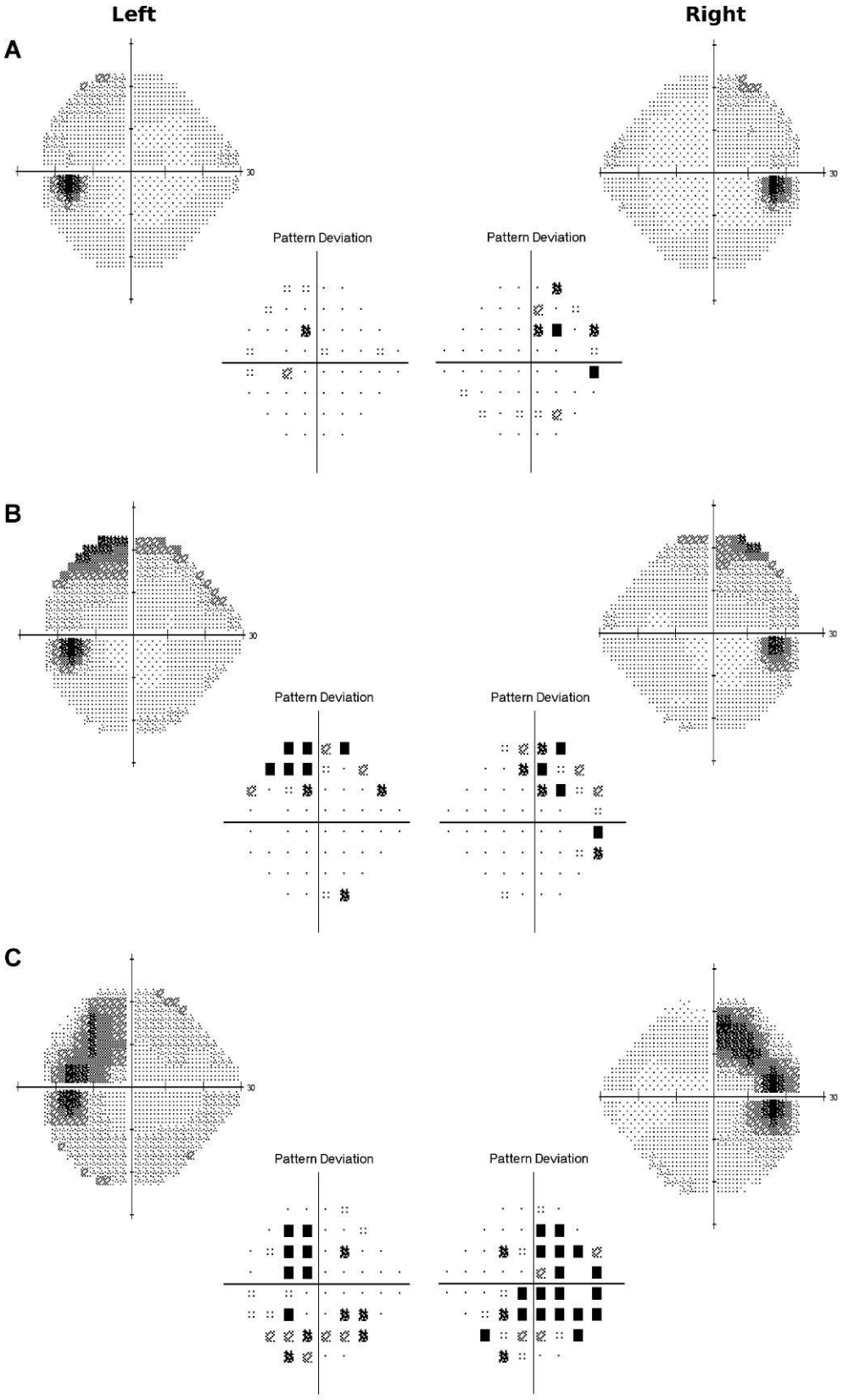

FIGURE 2. Examples of visual field defects caused by chiasmal injury. (**A**) A subtle example of a bitemporal defect with a maximum NHT score of 40. (**B**) An example of a bitemporal defect with more significant abnormalities in a number of individual test locations, but with the same NHT score of 40 as the example in (**A**), due to abnormal points in the "unaffected" hemifield. (**C**) An example of a bitemporal defect with an NHT score of 51.

Investigative Ophthalmology & Visual Science

Table 3. Summary of ROC Analysis for the Various NHT Parameters Using Training and Validation Datasets

	Training, $n = 474$		Validation, $n = 159$	
Predictors	**AUC**	**95% CI**	**AUC**	**95% CI**
NHT maximum	0.88	0.85, 0.92	0.92	0.87, 0.97
NHT sum	0.89	0.86, 0.92	0.92	0.87, 0.97
NHT laterality right and left	0.69	0.64, 0.75	0.68	0.58, 0.78
NHT sum, NHT laterality right and left	0.92	0.89, 0.95	0.93	0.88, 0.98

Table 4. Summary of ROC Analysis for the Machine Learning Classifiers Using Training and Validation Datasets

	Training, $n = 474$		Testing, $n = 159$	
Algorithm	**AUC**	**95% CI**	**AUC**	**95% CI**
Decision tree	0.95	0.93, 0.97	0.90	0.84, 0.96
Random forest	1.00	1.00, 1.00	0.95	0.92, 0.99
LASSO	0.95	0.93, 0.97	0.96	0.92, 0.99

Table 5. Sensitivity and Specificity for Detection of Neurological Visual Fields in the Validation Data Using Different Cutoffs in the Value of the Maximum NHT Score Between Right and Left Eyes

NHT Maximum	Sensitivity	Specificity	PPV	NPV
30	0.89	0.72	0.62	0.93
35	0.87	0.78	0.67	0.92
40	0.85	0.84	0.73	0.91
50	0.83	0.91	0.81	0.91
55	0.79	0.95	0.89	0.90
65	0.77	0.97	0.93	0.89
70	0.75	0.98	0.95	0.89

Table 6. Distribution of Cases at Reasonable Cutoffs of the Maximum NHT Score Between Two Eyes or the Sum of the NHT Scores Between Two Eyes

Group	NHT Maximum <50	NHT Maximum ≥ 50	NHT Sum <70	NHT Sum ≥ 70
Neurological, *n* (%)	9 (17)	44 (83)	9 (17)	44 (83)
Glaucoma, *n* (%)	43 (81)	10 (19)	42 (70)	11 (20)
Suspect, *n* (%)	52 (98)	1 (2)	52 (98)	1 (2)

Table 7. Categorization of Neurological Cases Using a Combination of the NHT Laterality Score and NHT Score

Neurological Type Using Binocular NHT Scores	Neurological Type by Clinical Diagnosis		
	Bitemporal	**Left Homonymous**	**Right Homonymous**
Bitemporal, *n* (%)	31 (86)	0	0
Left homonymous, *n* (%)	0	75 (99)	0
Right homonymous, *n* (%)	5 (14)	0	52 (100)
Binasal, *n* (%)	0	1 (1)	0

each visual field quadrant at the beginning of the test will subsequently receive only bright stimuli directed to that quadrant. To "produce" a defect in that quadrant, one must respond only to dim lights and not to bright ones. Such artificially produced visual defects can be identical to true neurological defects, and neither a clinician nor the NHT would be able to determine that they were spurious without further clinical history and evaluation.

In summary, the NHT can distinguish chiasmal and postchiasmal visual field defects from defects caused by glaucoma, and compares favorably with the performance of subspecialists in discriminating neurological field defects. Using the visual field information from both eyes, it can also categorize the pattern as bitemporal or homonymous. We believe this test will be most useful in the general eye care setting, where neurological disease can be missed or mistaken for other eye disease. The algorithms discussed here have the potential to be included on perimetry machines and incorporated into clinical practice.

Acknowledgments

Supported in part by NEI Grant EY01765 (Core Facility Grant, Wilmer Institute); a Heed Fellowship (ANM); funds from the Leonard Wagner Trust, New York, New York; Saranne and Livingston Kosberg; William T. Forrester; and a grant to the Wilmer Eye Institute from Research to Prevent Blindness.

Disclosure: **A.N. McCoy**, None; **H.A. Quigley**, Carl Zeiss Meditec (C); **J. Wang**, None; **N.R. Miller**, None; **P.S. Subramanian**, None; **P.Y. Ramulu**, Carl Zeiss Meditec (C); **M.V. Boland**, Carl Zeiss Meditec (C)

References

1. Asman P, Heijl A. Glaucoma hemifield test. Automated visual field evaluation. *Arch Ophthalmol*. 1992;110:812–819.
2. Asman P, Heijl A. Evaluation of methods for automated hemifield analysis in perimetry. *Arch Ophthalmol*. 1992;110: 830–836.
3. Lietman T, Eng J, Katz J, Quigley HA. Neural networks for visual field analysis: how do they compare with other algorithms? *J Glaucoma*. 1999;8:77–80.
4. Goldbaum MH, Sample PA, White H, et al. Interpretation of automated perimetry for glaucoma by neural network. *Invest Ophthalmol Vis Sci*. 1994;35:3362–3373.
5. Bizios D, Heijl A, Bengtsson B. Trained artificial neural network for glaucoma diagnosis using visual field data: a comparison with conventional algorithms. *J Glaucoma*. 2007;16:20–28.
6. Goldbaum MH, Lee I, Jang G, et al. Progression of patterns (POP): a machine classifier algorithm to identify glaucoma progression in visual fields. *Invest Ophthalmol Vis Sci*. 2012; 53:6557–6567.
7. Bowd C, Lee I, Goldbaum MH, et al. Predicting glaucomatous progression in glaucoma suspect eyes using relevance vector machine classifiers for combined structural and functional measurements. *Invest Ophthalmol Vis Sci*. 2012;53:2382–2389.
8. Bowd C, Hao J, Tavares IM, et al. Bayesian machine learning classifiers for combining structural and functional measurements to classify healthy and glaucomatous eyes. *Invest Ophthalmol Vis Sci*. 2008;49:945–953.
9. Kymes SM, Lambert DL, Lee PP, et al. The development of a decision analytic model of changes in mean deviation in people with glaucoma: the COA model. *Ophthalmology*. 2012; 119:1367–1374.
10. Strouthidis NG, Scott A, Viswanathan AC, Crabb DP, Garway-Heath DF. Monitoring glaucomatous visual field progression: the effect of a novel spatial filter. *Invest Ophthalmol Vis Sci*. 2007;48:251–257.
11. Boland MV, McCoy AN, Quigley HA, et al. Evaluation of an algorithm for detecting visual field defects due to chiasmal and postchiasmal lesions: the neurological hemifield test. *Invest Ophthalmol Vis Sci*. 2011;52:7959–7965.
12. Bunt AH, Minckler DS, Johanson GW. Demonstration of bilateral projection of the central retina of the monkey with horseradish peroxidase neuronography. *J Comp Neurol*. 1977; 171:619–630.
13. Katz J, Quigley HA, Sommer A. Detection of incident field loss using the glaucoma hemifield test. *Ophthalmology*. 1996;103: 657–663.
14. Katz J, Quigley HA, Sommer A. Repeatability of the glaucoma hemifield test in automated perimetry. *Invest Ophthalmol Vis Sci*. 1995;136:1658–1664.
15. Boland MV, Quigley HA. Evaluation of a combined index of optic nerve structure and function for glaucoma diagnosis. *BMC Ophthalmol*. 2011;11:6.
16. Jaimes F, Farbiarz J, Alvarez D, Martínez C. Comparison between logistic regression and neural networks to predict death in patients with suspected sepsis in the emergency room. *Crit Care*. 2005;9:R150–R156.
17. Pasha T, Gabriel S, Therneau T, Dickson ER, Lindor KD. Cost-effectiveness of ultrasound-guided liver biopsy. *Hepatology*. 1998;27:1220–1226.
18. Svetnik V, Liaw A, Tong C, Culberson JC, Sheridan RP, Feuston BP. Random forest: a classification and regression tool for compound classification and QSAR modeling. *J Chem Inf Comput Sci*. 2003;43:1947–1958.
19. Friedman J, Hastie T, Tibshirani R. Regularization paths for generalized linear models via coordinate descent. *J Stat Softw*. 2010;33:1–22.
20. DeLong ER, DeLong DM, Clarke-Pearson DL. Comparing the areas under two or more correlated receiver operating characteristic curves: a nonparametric approach. *Biometrics*. 1988;44:837–845.
21. Glovinsky Y, Quigley HA, Bissett RA, Miller NR. Artificially produced quadrantanopsia in computed visual field testing. *Am J Ophthalmol*. 1990;110:90–91.

Investigative Ophthalmology & Visual Science